Available online at www.sciencedirect.com

ScienceDirect

Physics Procedia 60 (2014) 2 – 14

Physics Procedia

3rd International Meeting of the Union for Compact Accelerator-driven Neutron Sources, UCANS III, 31 July–3 August 2012, Bilbao, Spain & the 4th International Meeting of the Union for Compact Accelerator-driven Neutron Sources, UCANS IV, 23-27 September 2013, Sapporo, Hokkaido, Japan

# Use of the ESS Bilbao installations for laser fusion studies

Ángel R. Páramo[a], Fernando Sordo[a,b], Antonio Rivera[a], José Manuel Perlado[a]

[a]*Instituto de Fusión Nuclear UPM, José Gutiérrez Abascal 2, E28006 Madrid, Spain*
[b]*Consorcio ESS-Bilbao. Edificio Cosimet. Paseo Landabarri, 2 1a planta - 48940 Leioa (SPAIN)*

**Abstract**

In this work the use of ESS-Bilbao fast neutron lines for irradiation of materials for nuclear fusion is studied. For the comparison of ESS-Bilbao with an inertial fusion facility a simplified model of HiPER chamber has been used. Several positions for irradiation at ESS-Bilbao have been also compared.

The material chosen for the damage analysis is silica due to its importance on ICF optics. In this work a detailed comparison between the two facilities for silica irradiation is given. The comparison covers the neutron fluxes, doses, defect production and PKA spectra.

This study is also intended as a methodological approach or guideline for future works on other materials.



Peer-review under responsibility of the Organizing Committee of UCANS III and UCANS IV

*Keywords:* ESS-Bilbao, inertial fusion, final optics, silica lenses, radiation-induced damage.

## 1. Introduction

Nowadays, the National Ignition Facility (NIF) is devoting its efforts to the demonstration of fusion laser ignition. Achieving this milestone proving scientific feasibility of ICF (Inertial Confinement Fusion) combined to the advances that will be attained on plasma physics in ITER ( International Thermonuclear Experimental Reactor) will put nuclear fusion on the main front for the next few years. Other projects such as HiPER (Eu), Laser Mega-Joule (Fr) or LIFE (USA, Laser Inertial Fusion Energy) are aiming their efforts in the same direction.

* Corresponding author. Tel.: +34-91-336-31-26 ; fax: +34-91-336-30-02.
*E-mail address:* angel.rodriguez.paramo@upm.es



Peer-review under responsibility of the Organizing Committee of UCANS III and UCANS IV
doi:10.1016/j.phpro.2014.11.003

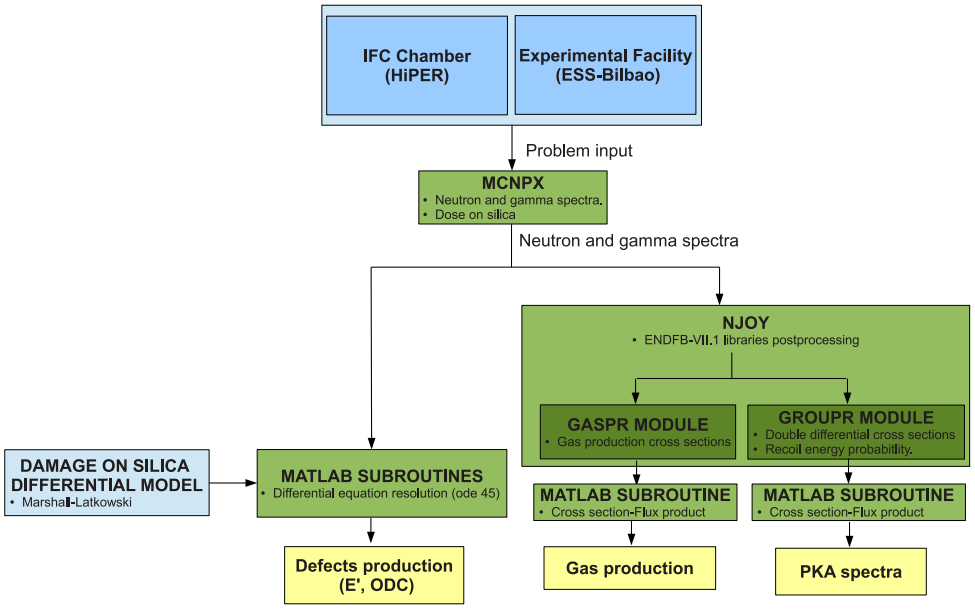


Fig. 1. Codes and subroutines used for the analysis presented in this work.

The HiPER project (High Power Laser Energy Research Facility) is now on its preparatory phase and its goal is to build an engineering facility for repetitive laser operation.

On the other side ESS-Bilbao is an accelerator driven compact neutron source under construction on the Leioa campus of the UPV/EHU (Universidad del Pais Vasco/Euskal Herriko Universitatea) near Bilbao (Basque Country, Spain) which is scheduled to begin operation $\sim$ 2020.

One critical problem of nuclear fusion is the lack of irradiation facilities that provide fusion neutrons (14.1 MeV). Most of the experiments are carried out with fission neutron sources with neutrons of $\sim$ 1 MeV average. On ESS-Bilbao, the neutron spectra will be more energetic, and better approximations to the fusion neutron spectra can be obtained.

Physical models for defect production can be improved at ESS-Bilbao. For the improvement of the physical models several fields have to be studied: gas production, displacement cascade size, energy available for defects, colour centre formation, etc.

For the study of such parameters, the PKA (Primary Knock-on Atom) spectra produced by the facility have to be studied for the materials of interest. In this work a comparison of between PKA spectra expected with relevant ICF conditions and at the ESS Bilbao facility is supplied. The PKA spectra gives a valuable input for MD (Molecular Dynamics) simulations covering defect production. The PKA spectra will also be needed by experimentalists in order to extrapolate their results and construct their physical models.

Finally an estimation of the defect production for silica is given. This estimation (based on experimental data from ref. Latkowski et al. (2003)) is given as an example of the physical models that could be developed or improved at an installation such as ESS-Bilbao.

## 2. Methodology

In this work the damage on silica under neutron irradiation is studied for an ICF chamber of 50 MJ and several positions at ESS-Bilbao. Several tools have been used: MCNPX Pelowitx et al. (2007) has been used for the calculation of neutron and gamma fluxes and doses on the lenses, NJOY Macfarlane et al. (2000) code has been used for the post-processing of nuclear libraries (ENDFB-VII.1 Chadwick et al. (2006)), and Matlab has been used for the resolution of the differential equations of the damage model and the product of the neutron flux (from MCNPX) and post-processed cross sections (from NJOY). A schema of the different steps followed in the present analysis is shown in Figure 1.

Apart from the tools described above, perl scripts have been used to process of ASCII files, and gnuplot to plot the results.

## 3. Inertial Confinement Fusion

In nuclear fusion the energy is produced by the deuterium-tritium fusion:

$$D_1^2 + T_1^3 \rightarrow He_2^4(3.5MeV) + n_0^1(14.1MeV) \qquad Q_c = 3.5MeV \tag{1}$$

In the inertial fusion scheme the high density of the plasma leads to significant neutron moderation that produces a shift in the neutron spectra to lower energies. The neutron spectrum used for the present analysis has been obtained from the Aries project Aries Webpage (2012).

### *3.1. Silica lenses at ICF chambers*

Silica lenses are a key component for the operation of an ICF reactor. The final lenses play a major role in laser optics, focusing the laser beams onto the target. Focusing errors lead to instabilities in the plasma and the impossibility of attaining ignition.

From the focusing point of view, current studies on final optics for HiPER propose to locate them 8 m away from the chamber centre. However, such a good location from the focusing point of view (see Figure 2) makes the lenses very exposed to severe irradiation conditions with detrimental consequences.

In the facilities where inertial fusion experiments are carried out, lenses are not exposed to continuous irradiation ($\sim$ 1 shot/day) and the detrimental effects of continuous irradiation do not appear. However for future experimental or demonstration plants with continuous operation ($\sim 1-20$ Hz), several effects complicate the lens performance. Those are the problems partially covered in this work and where experimental facilities can play a major role to assess the lifetime of the lenses.

To allow for a comparison between the different scenarios, a target of **50 MJ** corresponding to reactor HiPER prototype [1] has been simulated in all cases. In addition, the repetition chosen is 1 Hz.

## 4. ESS-Bilbao

ESS-Bilbao is a scientific facility that will be constructed at Leioa campus (Universidad del Pais Vasco, UPV) near Bilbao (Basque Country, Spain). ESS-Bilbao will be composed of a proton irradiation facility, a neutron compact

[1] $\sim$ 50 MJ is also the target energy for the LIFE.1 project. The LIFE.1 project is conceived as the first demonstration power plant of ICF, LIFE is based on a developed design of the National Ignition Facility (NIF).

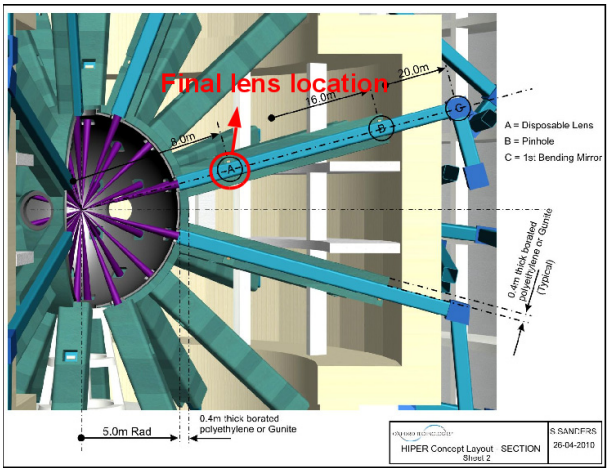


Fig. 2. HiPER ICF chamber and final lens position (8 m away from the centre.). Figure from Oxford Technologies.

source and will be used as a test facility for the ESS project. It is on the neutron compact source that this project is centred.

The neutron compact source is composed by the protons accelerator line, the target and the neutron lines. The accelerator is composed by the ions source ($H^+$ or $H^-$), a RFQ quadrupole and finally a DTL accelerator that accelerate the protons to 50 MeV.

The 50 MeV protons are directed through a transfer line to the beryllium target. On the beryllium target, the protons impact producing neutrons through stripping. The main reactions producing neutrons is:

$$^9Be + p \rightarrow {}^9B + n \tag{2}$$

Several applications are foreseen for the neutrons as a function of their energy (cold, thermal and fast). In this study the applications with fast neutrons are studied.

At the fast neutrons line, the sample positions will have to be installed near the target to have high neutron fluencies. Four positions are studied with MCNPX for the neutrons irradiation (see Figure 3):

- Pos. 1 and Pos 2. : on the thermal neutron line (at 45 ° [2] ) at 10 cm and 20 cm away from the target respectively.
- Pos. 3 and Pos 4. : on the fast neutron line (behind the target) at 10 cm and 20 cm away from the target respectively.

From the four positions, this study will be centred on **position 4** as it is the most likely to be used. In all the cases, the flux of particles is obtained for an incident proton current of 2.25 mA at 50 MeV (approx. 75 mA peak, 30 Hz, 1.5 ms width).

For the analysis of neutron and gamma fluxes and doses at the different positions, a MCNPX model with ENDFB-VII.1 libraries has been used Terrón et al. (2012).

[2] The neutron moderator will be installed at these positions, and they will not be available in principle for sample irradiation. In this study these two positions are shown to present the angular distribution in the chamber.

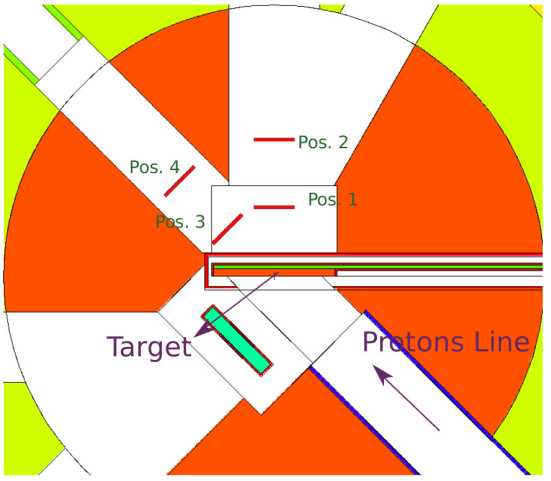


Fig. 3. MCNPX model of the ESS-Bilbao neutron target (model from GBAN Terrón et al. (2012)).

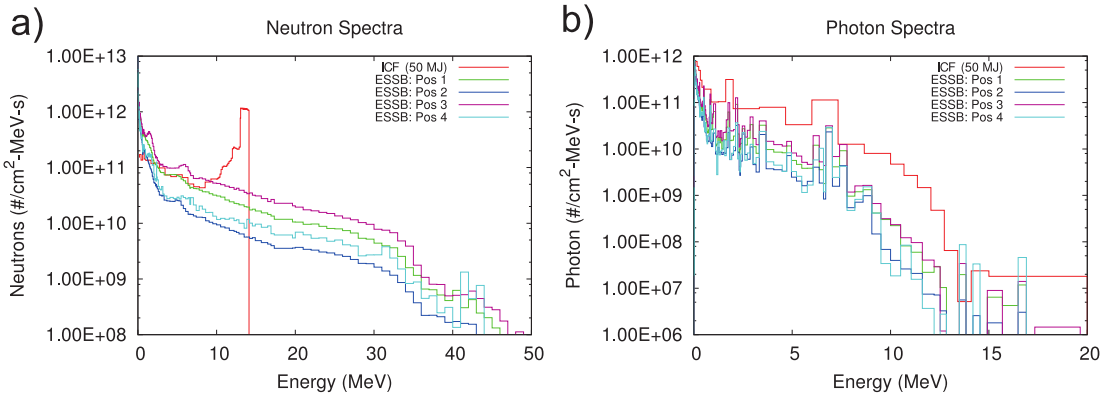


Fig. 4. Comparison of the neutron spectra at ESS-Bilbao and an ICF facility. Neutron (a) and gamma (b) fluxes in an ICF chamber (50 MJ, 1 Hz) and ESS-Bilbao at different positions are compared.

## 5. ICF and ESSB Comparison

### *5.1. Neutron and gamma fluxes*

For the different cases studied (ICF (50 MJ), ESSB Pos. 1, ESSB Pos. 2 , ESSB Pos. 3, ESSB Pos. 4 ) the neutron and gamma fluxes are shown on Figure 4 and Table 1 [3].

[3] In Table 1 only the neutrons with energies higher than 0.5 MeV have been integrated to give a representative estimation of the spectra average energy. The neutrons with lower energy are ~ 60% of the total but account only for ~ 5% of the deposited energy. For deposited dose and damage effect, the low energy neutrons can be rejected.

Table 1. Comparison of the neutron spectra at an ICF facility (50 MJ, 1 Hz) and ESS-Bilbao.

| | ICF (50 MJ) | ESSB 1 | ESSB 2 | ESSB 3 | ESSB 4 | ESSB4/ICF |
|---|---|---|---|---|---|---|
| Neutron (/cm$^2$s) | $2.50 \times 10^{12}$ | $1.20 \times 10^{12}$ | $4.77 \times 10^{11}$ | $1.83 \times 10^{12}$ | $6.54 \times 10^{11}$ | 26% |
| Average energy (MeV/n) | 10.14 | 7.01 | 5.97 | 7.87 | 6.92 | 68% |

### *5.2. Neutron and gamma doses*

The dose rates deposited in the silica sample are given in Table 2. It is observed that the dose for the position 4 of ESS-Bilbao is ∼ 15% of the dose in the ICF chamber. This way 6.6 h of irradiation at ESSB pos. 4 would be similar to 1 h irradiation at an ICF facility (50 MJ, 1 Hz). In the following paragraphs a description of how the dose is deposited in the samples is given.

Considering the different reactions, at low neutron energies ($\lesssim$ 5 MeV) elastic reactions are dominant. For higher energies, inelastic and light charged particle production reactions become important (see Figure 5).

It is interesting to treat the recoil and light particle doses separately due to their different interaction mechanisms with matter:

- Recoil nuclei are heavy and they lose much of its energy in every interaction. Therefore, the secondary recoil nuclei have enough energy to form a displacement cascade.
- The light particles are stopped continuously by matter, and only a small fraction of their energy is lost in every interaction. Therefore, the secondary recoil nuclei will not have enough energy to form displacement cascades in this case.

With these considerations, in the present work only the recoil nuclei will be included to account for defect formation (see Table 2 [4]). On the other hand the total dose (recoils + light charged particles) has to be included for thermo-mechanical analysis.

The dose ratio of ESS-Bilbao to ICF (50 MJ, 1 Hz) is similar for the different reactions (Table 2). As the dose rates are similar in the different cases, the damage pattern will be similar and useful conclusions on material damage can be obtained at ESS-Bilbao. The difference in the dose rate (∼ 15%) can be compensated by having longer irradiation times at ESS-Bilbao.

Table 2. Dose rates for silica lenses at ICF (50 MJ, 1 Hz) and ESS-Bilbao. The dose is divided between the energy of the recoil nucleus from neutron collision, from gamma collisions and the energy of the light charged particles.

| | ICF (50 MJ) | ESSB 1 | ESSB 2 | ESSB 3 | ESSB 4 | ESSB4/ICF |
|---|---|---|---|---|---|---|
| Recoil Dose rate (Gy/s) | 12.4 | 4.1 | 1.5 | 6.7 | 2.2 | 17.85% |
| Gamma dose rate (Gy/s) | 8.2 | 1.4 | 0.8 | 1.9 | 0.9 | 11.10% |
| Protons dose rate (Gy/s) | 3.5 | 1.2 | 0.3 | 1.9 | 0.6 | 16.37% |
| Alpha dose rate (Gy/s) | 7.3 | 1.6 | 0.5 | 2.6 | 0.7 | 9.37% |
| Total dose rate (Gy/s) | 31.50 | 8.7 | 3.2 | 13.5 | 4.5 | 14.44% |

[4] Only the most relevant particles (recoil, gamma, protons and alphas) have been included in Table 2. The total dose rate includes energy from all rest of particles (deuterons, tritions, etc), this fact explains the small disagreement between the sum of the different particles dose rate and the total dose rate.

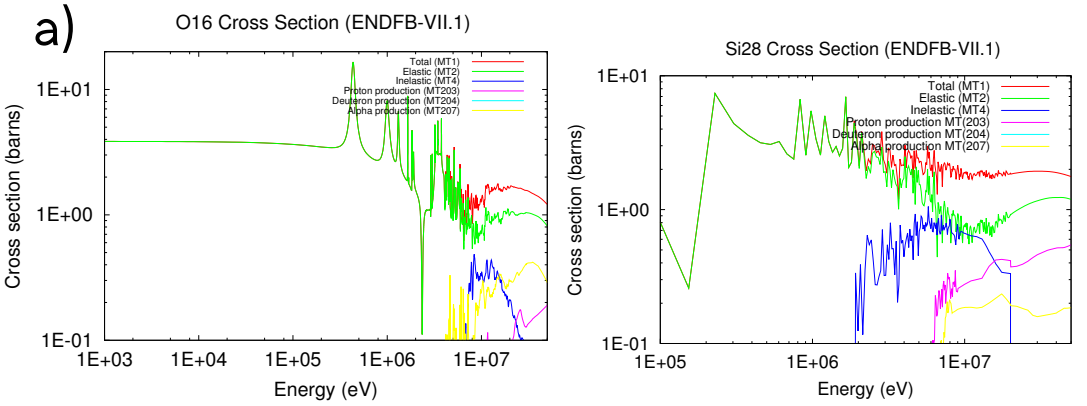


Fig. 5. $^{16}O$ (a) and $^{28}Si$ (b) cross sections for the different types of reactions. From the cross section it is clearly observed that for high energies ($\gtrsim$ 5 MeV ) non-elastic reactions appear, this has an effect on the energy of recoils, gamma emissions and gases production.

### 5.3. Gas Production

Figure 5 and Table 2 show that reactions involving light particles production (protons and alphas) are important for the neutron-silica interaction [5]. On Table 3 light particle production [6] for the different elements ($^{16}O$,$^{28}Si$) is presented.

Table 3. Gas production in silica given as parts per million per year (ppm/year) of total atoms.

| | ICF (50 MJ) | ESSB4 | ESSB4/ICF |
|---|---|---|---|
| $^{16}O$: Protons (appm/year) | 1.4 | 0.3 | 17.9% |
| $^{16}O$: Alphas (appm/year) | 9.4 | 1.2 | 13.2% |
| $^{28}Si$: Protons (appm/year) | 6.3 | 0.8 | 13.1% |
| $^{28}Si$: Alphas (appm/year) | 3.7 | 0.4 | 11.3% |
| Total: Protons (appm/year) | 7.7 | 1.1 | 13.9% |
| Total: Alphas (appm/year) | 13.0 | 1.7 | 12.7% |

### 5.4. PKA spectra

As explained on section 5.2 the recoils are responsible for most of the damage. To give an accurate description of how the damage is induced, the PKA (Primary Knock-on Atom) spectra is necessary. The PKA spectra gives a description of the behaviour of the lenses to irradiation in the different facilities. The PKA spectra serves also as an input for MD (Molecular Dynamics) simulations.

For the study of the PKA spectra, double differential cross sections have been post-processed with the NJOY code Macfarlane et al. (2000). The post-processing is done with the module GROUPR, obtaining the (n,recoil) diffusion matrices; similar procedure has been already followed by other authors for the characterisation of other facilities (IFMIF, Demo, Technofusion) Simakov et al. (2009); Mota et al. (2011).

[5] The gas production cross sections have been obtained from post-processing of ENDFB-VII.1 with NJOY code and its GASPR module.

[6] The results have been expressed as particles per million per year (ppm/year) of an average silica atom. One atom of silica is composed of 0.66 atoms of $^{16}O$ and 0.33 atoms of $^{28}Si$; and has a mass of 20 g/mol

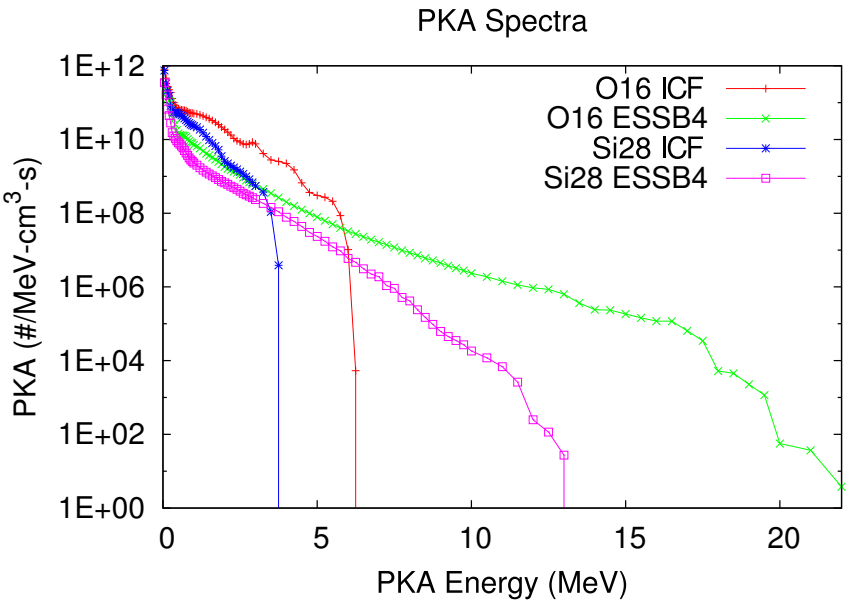


Fig. 6. PKA spectra for ICF (50 MJ, 1 Hz) and ESSB4 (2.25 mA, 30 Hz).

Figure 6 shows the PKA spectra for $^{16}O$ and $^{28}Si$. PKAs of $^{16}O$ are more energetic than the PKAs of $^{28}Si$ due to their lower mass. It is clearly observed how the maximum energy is higher at ESS-Bilbao (where neutrons up to 50 MeV could appear) than on ICF (neutrons up to 14.1 MeV). The presence of this high energy PKAs could lead to several effect. These effect are difficult to measure without experimental data as usually opposed effects appear at high energies:

- At high PKAs energies electronic stopping power appearance would decrease the damage. However electronic damage could appear. The electronic damage is produced for stopping powers exceeding a threshold value, typically around 2 keV/nm for silica. Such a threshold is typical for heavy charged particles (energy-mass ratio > 0.1 MeV/amu) Rivera et al. (2008).
- Also at high PKA energies high temperatures that are attained on the area surrounding the PKA. These high temperatures could lead to annealing of defects. However with higher PKAs energy, the cascade size is bigger which limits the defects annealing.

Even with the differences in the PKA spectra for ICF and ESS-Bilbao, an analysis on Figure 6 shows that a similar pattern is followed. Based on this similar pattern it can be concluded that with the correct extrapolations or spectra shaping [7] at ESS-Bilbao, valuable results could be obtained.

[7] Spectra shaping includes the operations to adapt the ESS-Bilbao spectra to a fusion spectra (moderator, absorption windows, etc).

## 6. Colour centre formation

### 6.1. Defect formation

When matter is subjected to irradiation, defects are formed in its structure. When a neutron collides with matter it creates a PKA (primary knock-atom). The PKA leaves its original position and collides with atoms of the lattice creating secondary recoils and forming a displacement cascade. During the displacement cascade the defects can recombine forming a complex mechanism; molecular dynamics (MD) or models can be used to determine the final number of defects. In this study a model proposed by Marshall Marshall et al. (1997) and reviewed by Latkowsky Latkowski et al. (2003) based on experimental data will be used for the defect production calculation.

The defect production estimation is given as an example of the physical models that could be developed or improved with new experimental data at ESS-Bilbao.

### 6.2. Defects on silica

The silica is a fourfold structure that can be subjected to different types of defects. The most interesting defects for the optics at ICF are the ODC (Oxygen Defect Centre) and E'. These defects produce colour centres with light absorption on the range of the ICF laser (350 nm). This laser absorption would complicate laser focusing.

The typical structure of $SiO_2$, is a 4-fold bond, with each $Si$ bonded to 4 oxygensKubota et al. (2002). When an oxygen is displaced, a 3-fold on the Si is formed, with the resting covalent bond between two Si atoms. Different defects and final configurations are possible, but in this work Oxygen Defect Centres (ODC) and associated defects (E') are studied.

When silica is irradiated with neutron irradiation an oxigen can be displaced forming a Si-Si bond (Oxygen Defect Center) and Si-O O-Si bonds (Non Bridged Oxygen Hole Center, NBOHC). This Si-Si bond can be broken due to gamma irradiation resulting in a E' center. Finally E' and NBOHC defects are subjected to thermal annealing. This mechanism of defects is described by Marshall and Latkowsky in Refs. Latkowski et al. (2003); Marshall et al. (1997), where an analytical model for the calculation of the color centres is given. More information about silica defects can be found at Kubota et al. (2002); Griscom (1991); Skuja et al. (2012).

### 6.3. Model description

In this section the model described by Marshall and Latkowsky Marshall et al. (1997); Latkowski et al. (2003) is presented; with this model the number of ODC and E' defects and the associated absorption coefficient have been studied.

#### 6.3.1. Lenses absorption

The total absorption coefficient can be calculated as:

$$\alpha(\lambda) = \sum_i \sigma_i N_i L_i(\lambda) = \sum_i \alpha_i L_i(\lambda) \tag{3}$$

$$L_i(\lambda) = \frac{1}{1 + \frac{(\lambda_i - \lambda)^2}{(\Delta\lambda_i)^2}} \tag{4}$$

The inclusion of $L_i(\lambda)$ comes from the Lorentzian approximation of the microscopic absorption coefficient ($\sigma_i(\lambda)$):

$$\sigma_i(\lambda) \approx \sigma_i \cdot L_i(\lambda) \tag{5}$$

Defect concentration can be defined as:

$$\frac{dN_{ODC}}{dt} = M_n \cdot D_n - \beta_{E'} \cdot D_\gamma \cdot N_{ODC} - \frac{N_{ODC}}{\tau_{ODC}} \tag{6}$$

$$\frac{dN_{E'}}{dt} = \beta_{E'} \cdot D_\gamma \cdot N_{ODC} - \frac{N_{E'}}{\tau_{E'}} \tag{7}$$

Where: $\alpha_i$ is the absorption coefficient of a defect $i$. $\sigma_i$ is defect centre cross section of a defect $i$. $N_i$ is the defect concentration. $L(\lambda)_i$ is the factor to account for the width of the defect centre. $\lambda$ is the light wavelength. $\lambda_i$ is the peak wavelength for the defect centre $i$. $\Delta\lambda_i$ is the half width at half maximum of the wavelength for the centre $i$. $\tau$ is the annealing time. $M_n$ is the number of defects following a PKA. $\beta_E$ is the cross section for ODC-E' conversion ($Gy^{-1}$). $D_\gamma$ is the gamma dose on the lenses. $D_n$ is the neutron dose on the lenses. $ODC$ is the oxygen defect centres. $E'$ is the electronic defects.

### *6.3.2. Parameters used for the model*

The values used for the parametric model are listed in Table 4.

For the estimation of the number of defects the following defects production factor is used (factor from ref. Latkowski et al. (2003)):

$$M_n = 0.37 \frac{defects}{\text{keV-PKA}} \tag{8}$$

This value was obtained from experimental results with neutron dose of $10^4$ Gy at Sandia National Laboratories (SNL) using the Annular Core Research Reactor (ACRR) Latkowski et al. (2003).

Table 4. Parameters for the defect production model.

| Parameter | Value | Ref. | Parameter | Value | Ref. | Parameter | Value | Ref. |
|---|---|---|---|---|---|---|---|---|
| $\sigma_{ODC}$ (cm$^2$) | $1.70 \times 10^{-17}$ | Latkowski et al. (2003) | $\sigma_{E'}$ (cm$^2$) | $3.20 \times 10^{-17}$ | Latkowski et al. (2003) | $\beta_E$ (Gy$^{-1}$) | $7 \times 10^{-5}$ | Latkowski et al. (2003) |
| $\lambda_{ODC}$ (nm) | 248 | Kuzuu (1994) | $\lambda_{E'}$ (nm) | 214 | Kuzuu (1994) | $\tau_0$ (s) | $4 \times 10^{-10}$ | Latkowski et al. (2003) |
| $\Delta\lambda_{ODC}$ (nm) | 13 | Kuzuu (1994) | $\Delta\lambda_{E'}$ (nm) | 15 | Kuzuu (1994) | $T_{anneal}$ (K) | 21000 | Latkowski et al. (2003) |

## *6.4. Model results*

The model has been run for an irradiation time of 1500 s; ICF (50 MJ) at 1 Hz and ESSB at 30 Hz (2.25 mA average current) [8].

On Figure 7 the absorption coefficient is shown for the different wavelengths. The absorption coefficient is higher at low temperature than at high temperature ($\sim 900K$) where the annealing term plays a significant role.

## *6.5. Model discussion*

The parameters of section 6.3.2 have been obtained from neutron spectra Latkowski et al. (2003); Marshall et al. (1997) different from ICF or ESS-Bilbao spectra. This model has several limitations that are discussed in the following paragraphs.

*Use of nuclear libraries.* In Refs. Marshall et al. (1997); Latkowski et al. (2003) the model is ideally implemented supposing that only elastic collisions take place. This fact approximates reality at low incident neutron energies, but do not result in accurate approximations for higher energies. In this work ENDFB-VII.1 nuclear libraries have been used including all type of reactions.

[8] As the frequency of the two cases (ICF, ESSB) is different, the number of simulated pulses changes. 1500 pulses have been simulated for ICF (1 Hz) and 45000 pulses for ESSB (30 Hz).

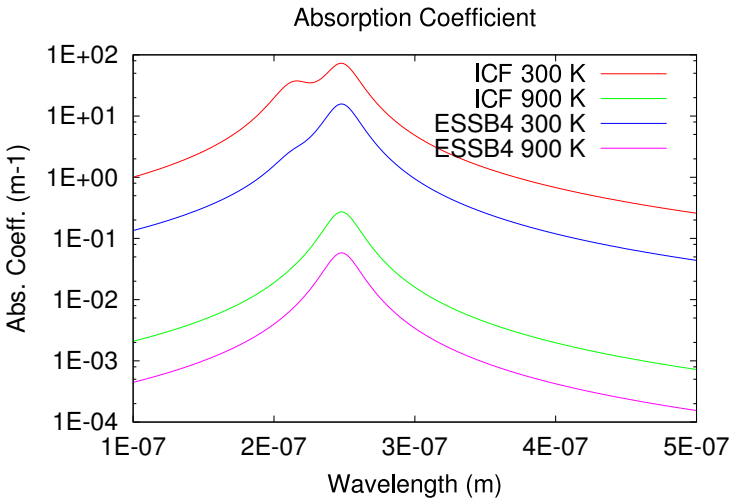


Fig. 7. Comparison of the absorption coefficient after 1500 s at ESSB pos. 4 (2.25 mA, 30 Hz) and an ICF chamber (50 MJ, 1 Hz).

*Gas production.* As can be observed on Figure 5 non-elastic reactions appear for neutron energies higher than $\sim 5-6$ MeV. These non-elastic collisions induce a change in the energy per collision (inelastic-reactions) and produce light charged particles (p,a). An analysis of the defects generated by light particles would result in an improvement on the model.

*Transmutation and impurities.* Although not given in this work, the transmutation of O and Si into other elements have an effect on the defects production. The transmuted atoms are likely to remain as interstitials altering mechanical properties and creating colour centres with effective light absorption on the ICF laser wavelength. The same conclusions can be applied to impurities in silica.

*Defect production.* In equation 8, a linear model for defect production is given. This is a simplification, not correct for high neutron energies. Also the physics of the defects is far from being completely understood and great improvements could be done in installations such as ESS-Bilbao.

*Defect saturation.* When high irradiation doses are applied on a material, a homogeneous defect distribution is attained on the sample. In these cases, when a new displacement cascade is created, the pre-existing defects may be annealed. This process would be caused by the high local temperatures in the area of the displacement cascade.

*Refraction index.* The refraction index determines the focusing characteristics of the lenses. In this study the aberrations that could appear from lens compaction due to irradiation have not been analysed. However when PKAs of high energy are produced after irradiation, a compaction of the affected zone leads to a variation in the refractive index Olivares et al. (2012). As has been seen in Figure 6, PKAs of high energy appear due to ICF or ESS-Bilbao fluxes. Although the presence of these high energetic PKAs is low, special attention has to be paid to possible appearance of compacted areas where the refractive index changes.

*PKA spectra.* Due to the linearity of the employed model (see eq. 8) the PKA spectra shown in Figure 6 is not necessary for the calculation of the defects production. The total dose has been used as seen on equation 6.

As pointed out in the previous paragraphs, the linearity of defect production is a large simplification. A model for a better representation of the defect production, should take into account the variation of defect production as a function of the PKA energy. In such a case the PKA spectra should be used as an input for defect production, and equation 8:

$$\frac{dN_{ODC}}{dt} = M_n \cdot D_n - \beta_{E'} \cdot D_\gamma \cdot N_{ODC} - \frac{N_{ODC}}{\tau_{ODC}}$$

Should be transformed to:

$$\frac{dN_{ODC}}{dt} = \int_{E_{PKA}} M_n(E_{PKA}) \cdot E_{PKA} \cdot \phi_{EPKA}(E_{PKA}) dE_{PKA} - \beta_{E'} \cdot D_\gamma \cdot N_{ODC} - \frac{N_{ODC}}{\tau_{ODC}} \quad (9)$$

Where: $E_{PKA}$ is the energy of the PKA. $phi_{PKA}$ is the spectra of PKAs.

## 7. Conclusions

In this work a comparison of the fluxes (Figure 4), doses (Tables 2), PKA spectra (Figure 6) and defects (Figure 7) is shown for silica lenses at an ICF chamber and at ESS-Bilbao.

The comparison shows that although the dose rate on ESS-Bilbao is lower ($\sim$ 15%), the spectra can be compared. The dose of the different reactions is similar (see Table 2), gas production ratios are similar (see Table 3) and PKA spectra have similar shapes (see Figure 6). With this analysis it can be concluded that by scaling the irradiation time on ESS-Bilbao similar results and damage effects can be obtained. As a result, ESS-Bilbao can be a useful installation for nuclear fusion materials irradiation under realistic conditions.

The neutron energy is important on the defect production. Several factors as light charged production, displacement cascade size or energy available for defects, are dependant on neutron energy. In facilities where materials are tested usually the average neutron energy is around 1 MeV while on ESS-Bilbao the spectra is significantly more energetic. Based on this it is possible to improve models of defect generation mechanisms at ESS-Bilbao. Shaping the spectra with absorbers and moderators would also allow for more accurate studies of the defect mechanisms. This way the effect of the energy on the defects production could be analysed.

As the PKA spectra obtained in ESS-Bilbao have a similar shape as those obtained in ICF (see Figure 6), it can be concluded that with the correct extrapolation or spectra shaping, valuable results on materials damage can be obtained at ESS-Bilbao. In section 6.5 a description of how existing models could be improved with new experimental data is given. The calculated PKAs are also a useful tool in order to design correctly the ESS-Bilbao fast neutron line. They also allow for a better understanding of the facility and the type of experiments that can be carried out. The knowledge of the PKA spectra allows experimentalists to evaluate their needs and design their experiments.

The study shows also the absorption coefficient for silica lenses at different temperatures (see 7), silica lenses have to be kept at high temperature (see ref. Garoz et al. (2013)) so that the rate of annealing is higher than the rate of defects creation. The mechanism of annealing is thought to be not well described, and factors such as impurities or the cascade size (related to the neutron spectra) could play a significant role. ESS-Bilbao could be used for such an analysis to have a better model of annealing and through a better understanding of phenomena better designs can be obtained.

Finally it is necessary to point out that although this study has been focused on silica lenses, it could be extrapolated to other materials, as the neutron fluxes would be the similar. Other materials where ESS-Bilbao could be useful for irradiation are:

- Breeding materials.

- Remote handling (electronics, single events failures).
- Superconducting materials.

## References

Latkowski Jeffery F., Payne Stephen A., et al. 2003. Fused silica final optics for inertial fusion energy: radiation studies and system-level analysis. Fusion Science and Technology as part of the Proceedings of the Nineteenth Topical Meeting on the Technology of Fusion Energy (TOFE), 43(540).

Denise. B. Pelowitx 2007. MCNPX User's Manual: Version 2.6.0.

Macfarlane, R. E. and Muir, D. W, 2000. NJOY99.0: Code System for Producing, Pointwise and Multigroup Neutron and Photon Cross Sections from ENDFB Data.

Chadwick, M. B., et al. 2006. ENDF/B-VII. 0: Next generation evaluated nuclear data library for nuclear science and technology. Nuclear Data Sheets 107.12.

Aries Webpage. http:aries.ucsd.edu/ARIES/WDOCS/ARIES-IFE/.

S. Terron, M. Magán, F. Sordo et al. 2012. Neutronic design for ESS-BILBAO neutron source. Technical report, ESS-BILBAO.

S.P. Simakov et al. 2009. Comparative study of survived displacement damage defects in iron irradiated in IFMIF and fusion power reactor Journal of Nuclear Materials.

F Mota, R Vila, C Ortiz et al. 2011. Analysis of displacement damage in materials in nuclear fusion facilities (DEMO, IFMIF and TechnoFusion). Fusion Engineering and Design, 86(6-8):2425(4).

A. Rivera, J. Olivares, G. Garcia, and F. Agullo-Lopez, 2008. Electronic-excitation versus nuclear collision damage by ion-beams in dielectric materials (LiNbO3). Nuclear Instruments and Methods in Physics Research Section B: Beam Interactions with Materials and Atoms, 266.

Christopher D. Marshall, Joel A. Speth, and Stephen A. Payne, 1997. Induced optical absorption in gamma, neutron and ultraviolet irradiated fused quartz and silica. Journal of Non-Crystalline Solids, 212(1):59–73.

A. Kubota, M.-J. Caturla, S.A. Payne, T. Diaz de la Rubia, and J.F. Latkowski, 2002. Modeling defect production in silica glass due to energetic recoils using molecular dynamics simulations. Journal of Nuclear Materials, 307-311, Part 2(0):891–894.

David L. Griscom 1991. Optical Properties and Structure of Defects in Silica Glass: Optical Materials. Journal of the Ceramic Society of Japan, 99(1154):923–942.

L. Skuja, K. Kajihara, M. Hirano, and H. Hosono, 2012. Oxygen-excess-related point defects in glassy/amorphous SiO2 and related materials. Nuclear Instruments and Methods in Physics Research Section B: Beam Interactions with Materials and Atoms.

Nobu Kuzuu, 1994. X-ray induced absorption bands in synthetic fused silicas: OH content dependence of intensities of X-ray-induced absorption bands in type-III fused silicas. Journal of Non-Crystalline Solids, 179(0)

J. Olivares A. Rivera O. Pena-Rodriguez and F. Agullo-Lopez, J. Manzano-Santamaria, 2012. Kinetics of color center formation in silica irradiated with swift heavy ions: Thresholding and formation efficiency. Applied Physics Letters 101.

Garoz, D., A. Rivera. et al. 2013. Silica final lens performance in laser fusion facilities: HiPER and LIFE. Nuclear Fusion 53, no. 1 (2013): 013010.